Science Advances
AAAS

advances.sciencemag.org/cgi/content/full/4/9/eaat5895/DC1

Supplementary Materials for

Evidence of a low-temperature dynamical transition in concentrated microgels

Marco Zanatta, Letizia Tavagnacco, Elena Buratti, Monica Bertoldo*, Francesca Natali, Ester Chiessi, Andrea Orecchini*, Emanuela Zaccarelli*

*Corresponding author. Email: monica.bertoldo@pi.ipcf.cnr.it (M.B.); andrea.orecchini@unipg.it (A.O.); emanuela.zaccarelli@cnr.it (E.Z.)

Published 28 September 2018, *Sci. Adv.* **4**, eaat5895 (2018)
DOI: 10.1126/sciadv.aat5895

This PDF file includes:

Section S1. EINS measurement and data analysis

The thermal protocol followed during the EINS measurements is reported in Tab. S1.

Table S1. Thermal protocol followed during the EINS measurements. Cooling (top part) and heating (bottom part) ratios used during the EINS measurements for each PNIPAM sample.

Step	T_i (K)	T_f (K)	43% (K/min)	50% (K/min)	60% (K/min)	70% (K/min)	95% (K/min)
1	288	283	0.7	0.3	0.7	0.6	0.3
2	283	253	0.8	0.6	0.8	0.8	0.6
3	253	233	0.7	0.5	0.7	0.7	0.5
4	233	218	0.6	0.4	0.6	0.6	0.4
5	218	203	0.6	0.4	0.6	0.6	0.4
6	203	188	0.6	0.4	0.6	0.5	0.4
7	188	173	0.5	0.4	0.6	0.5	0.4
8	173	153	0.7	0.5	0.7	0.7	0.5
9	153	203	1.2	1.7	1.2	1.2	
10	203	253	1.2	1.7	1.1	1.1	
11	253	263	0.4	0.7	0.4	0.4	
12	263	273	0.4	0.7	0.4	0.4	
13	273	283	0.4	0.7	0.4	0.4	

In the incoherent approximation, the elastic neutron scattering intensity $I(Q,\,0)$ can be described by the double-well model [3]. Within this approximation, hydrogen atoms are supposed to be dynamically equivalent and may jump between two distinct sites of different free energy. The elastic intensity can be thus written as:

$$I(Q,0) \;=\; \exp\left(-Q^2\left\langle \Delta u^2\right\rangle_{vib}\right)\left[1-2p_1p_2\left(1-\frac{\sin(Qd)}{Qd}\right)\right] \tag{1}$$

where p_1 and p_2 are the probabilities of finding the hydrogen atom, respectively, in the ground and excited state, $\left\langle \Delta u^2\right\rangle_{vib}$ corresponds to the vibrational mean square displacement of protons

rattling in the bottom of the wells, and d is the distance between the two wells. In this model, where a transition between the two states represents a jump between conformational substates in the free energy surface, the amplitude of the 3-dimensional mean squared displacement (MSD) is given by the relationship [38]:

$$\text{MSD} = -6\left(\frac{d\ln I(Q)}{dQ^2}\right)_{Q=0} = 6\left\langle \Delta u^2 \right\rangle_{vib} + 2p_1p_2d^2 \qquad (2)$$

Typical examples of the fits to the data with Eq. 1 are shown in Figs. S1 and S2 respectively for 43 wt % and 60 wt % samples. A pure D_2O sample was also measured to completely rule out the possibility of its crystallization in PNIPAM samples. Fig. S3 shows the $I(Q,0)$ for heavy water and for PNIPAM 43 wt % and 60 wt % at 153 K. PNIPAM samples do not show any traces of the D_2O Bragg peaks.

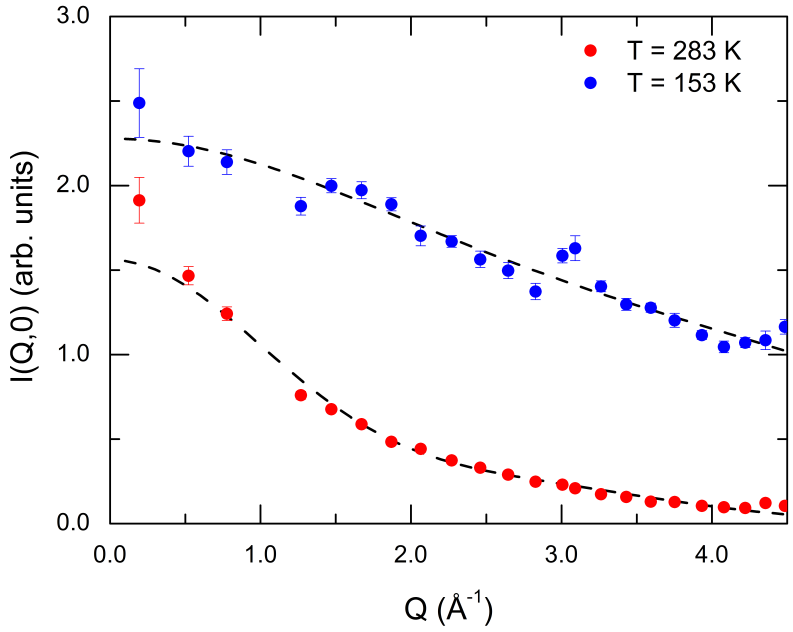

Fig. S1. **EINS data for PNIPAM 43 wt % sample.** $I(Q,0)$ measured on the PNIPAM 43 wt % sample at 283 K (red dots) and 153 K (blue dots); the black dashed line is the fit using Eq. 1.

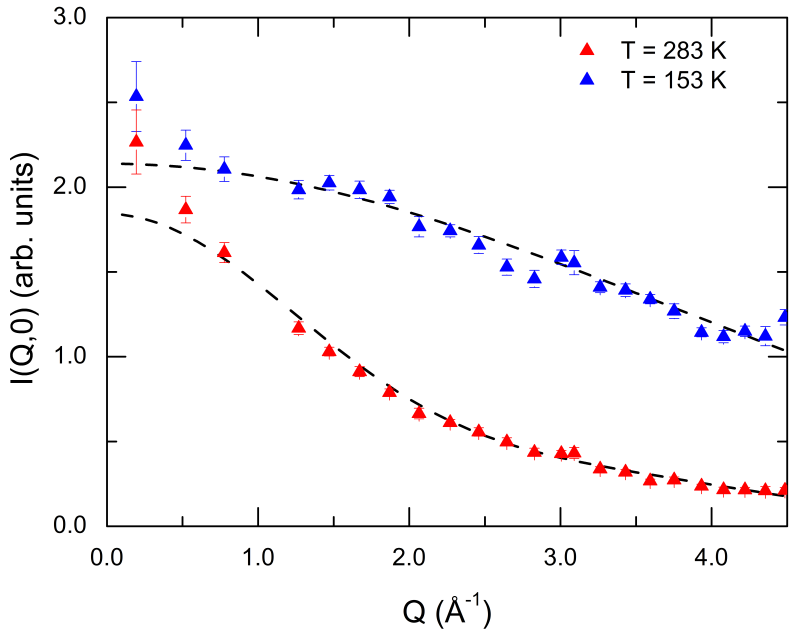

Fig. S2. **EINS data for PNIPAM 60 wt % sample.** $I(Q,0)$ measured on the PNIPAM 60 wt % sample at 283 K (red dots) and 153 K (blue dots); the black dashed line is the fit using Eq. 1.

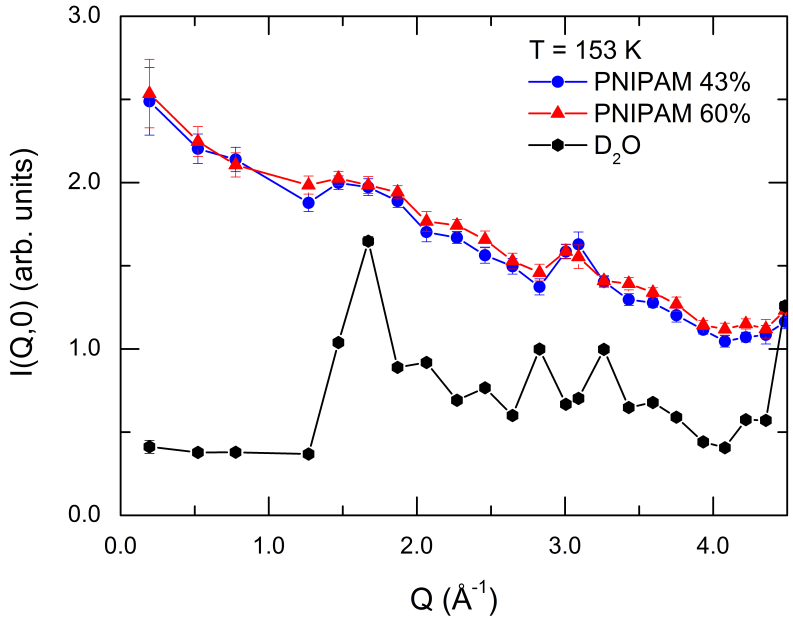

Fig. S3. **D_2O contribution to EINS spectra.** $I(Q,0)$ measured on pure D_2O compared with that obtained on PNIPAM samples with mass fraction of 43% and 60% at 153 K.

Section S2. PNIPAM model development

An isotropic polymer scaffold, with the network topology shown in Fig. S4, was built by cross-linking atactic PNIPAM chains in the minimum energy conformation [39]. Amide groups of PNIPAM residues were modeled in the trans conformation. Extra-boundaries covalent connectivity between polymer chains was applied. The network model includes 6 4-fold bis-acrylamide junctions and has a number average molecular weight of chains between cross-links, M_c, of 1584 g/mol, with a polydispersity index of 1.02. The average degree of polymerization of chains between junctions is 14 ± 2 .The polymer scaffold was hydrated by a shell of water molecules to set the PNIPAM concentration in the microgel. Then the system was equilibrated at 293 K in a pressure bath at 1 bar up to a constant density value, i.e. tot-drift less than 2×10^{-3} g cm^{-3} over 20 ns. A similar equilibration procedure was applied at each temperature before the NVT run.

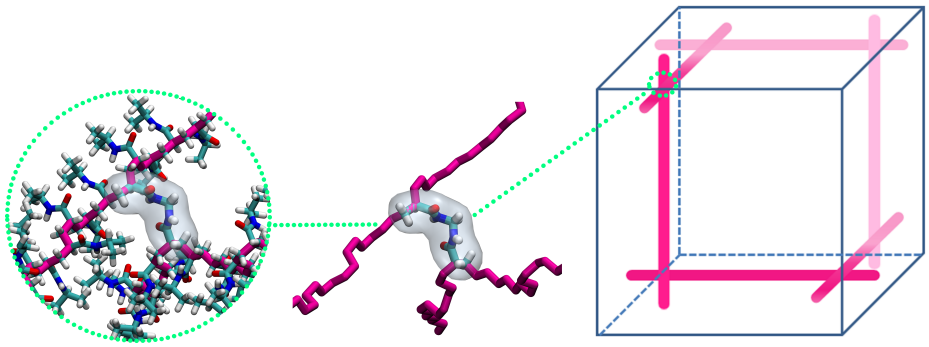

Fig. S4. **Schematic representation of the microgel network model.**

Section S3. MD simulations procedure

Molecular dynamics simulations of PNIPAM microgels were carried out using the GROMACS 5.0.4 software [40]. The polymer network was modeled using the OPLS-AA force field [41] with the implementation by Siu et al. [42], while water was described with the TIP4P/ICE model [30]. The system was equilibrated for 120 ns for $T \geq 273$ K and for 320 ns for $T \leq 263$ K in the NPT ensemble, taking into account the longer equilibration

time needed at lower temperatures. Simulation data were collected for 330 ns in the NVT ensemble, with a sampling of 0.2 frame/ps. The leapfrog integration algorithm was employed with a time step of 0.2 fs, cubic periodic boundary conditions, and minimum image convention. The length of bonds involving hydrogen atoms was kept fixed with the LINCS algorithm. The temperature was controlled with the velocity rescaling thermostat coupling algorithm with a time constant of 0.1 ps. Electrostatic interactions were treated with the smooth particle-mesh Ewald method with a cutoff of non-bonded interactions of 1 nm. The last 100 ns of trajectory were considered for analysis. The software MDANSE [43] as well as in-house codes were used for analysis of MD simulations to be compared with the neutron scattering data. Trajectory format manipulations (or conversions) were carried out by the software WORDOM [44]. The software VMD [45] was employed for graphical visualization.

Section S4. Reproducibility of numerical results

The numerical data are not affected by aging dynamics on the timescales investigated in the manuscript. To show that this is the case we report the evolution of the MSD upon changing the time interval for the calculation as well as waiting time t_w. Figure S5 shows the MSD of water oxygen atoms at the highest ($T = 293$ K) and lowest ($T = 223$ K) investigated temperatures. We calculate the MSD for a total time of 100 ns and compare it to the corresponding one calculated for only 10 ns (as used in the manuscript, Fig.2C). In addition, we also calculate it for $t_w = 0, 50, 90$ ns. All curves superimpose on the entire investigated timescale, in particular for the intermediate window where the self-diffusion coefficient was extracted, indicated by vertical dashed lines. This behaviour holds for both high and low temperatures. Similarly, Fig. S6 shows the MSD of PNIPAM hydrogen atoms at the same two temperatures over a total interval of 100 and 200 ns, the former being the ones from which we extract the value at 150 ps, reported in the manuscript in Fig. 4C. We also calculate it for waiting times $t_w = 0, 50, 100$ns. At long times, some differences, that are mostly attributable

to statistical error rather than aging, are visible. However, it is clear that for the timescale of relevance for comparison with experimental data, i.e. 150 ps, indicated by a vertical dashed line, no significant aging effects are found. This analysis ensures that the numerical data are reproducible and the system is well equilibrated for the short timescales studied in this work.

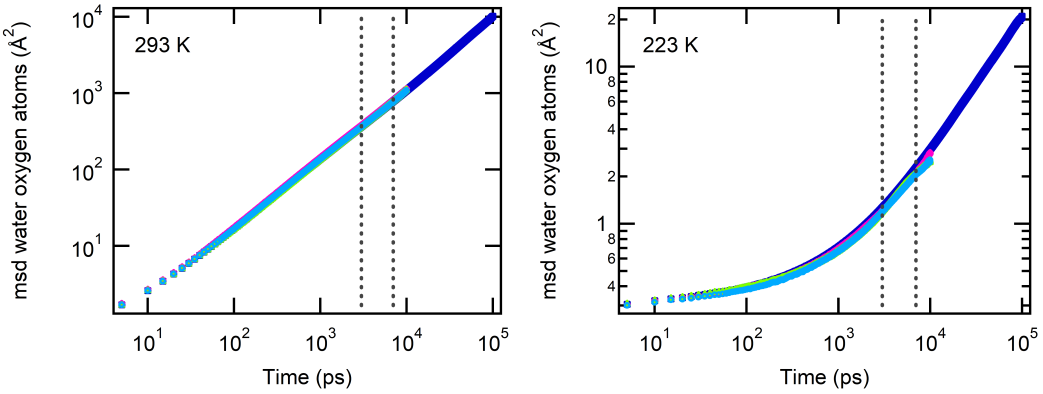

Fig. S5. **Aging effect on water dynamics.** Comparison between the mean square displacements of water oxygen atoms at 293 K (left panel) and 223 K (right panel) as calculated from the MD simulations over 100 ns of trajectory (blue squares), 0-10 ns (pink diamonds), 50-60 ns (green triangles), and 90-100 ns (light blue circles). Dashed lines highlight the linear region used for water diffusion coefficient calculation.

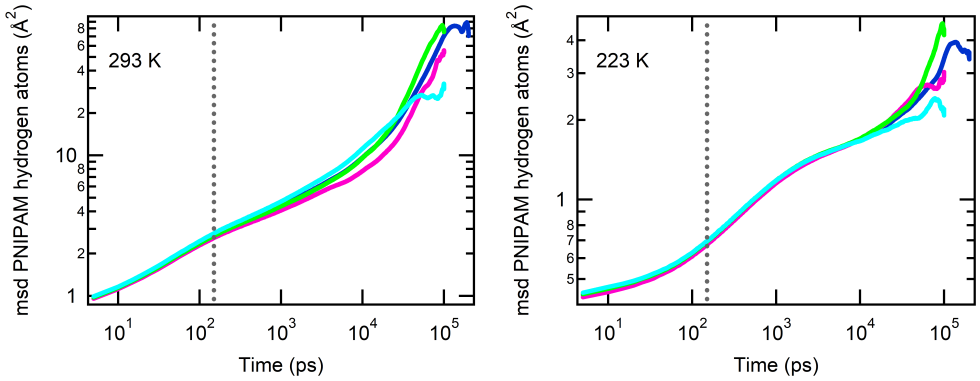

Fig. S6. **Aging effect on PNIPAM dynamics.** Comparison between the mean square displacements of PNIPAM hydrogen atoms at 293 K (left panel) and 223 K (right panel) as calculated from the MD simulations over 200 ns of trajectory (blue lines), 0-100 ns (pink lines), 50-150 ns (green lines), and 100-200 ns (light blue lines). The value at the experimental time resolution of 150 ps is indicated with a dashed line.

Section S5. Calculation of $I(Q,0)$ from numerical simulations

We have calculated both the coherent and incoherent intermediate scattering functions for all atoms in the simulations for wavevectors in the range $0.3 \leq Q \leq 4.5$ Å^{-1}. By summing the two contributions, weighted by the appropriate scattering lengths and by the partial concentrations, we have obtained the full differential cross- section. Its value at the experimental time resolution of 150 ps provides the numerical $I(Q,0)$.We have further checked that this procedure yields identical results as the calculation of the total dynamical structure factor (in frequency space) convoluted with the experimental resolution. An example of this procedure is provided in Fig.S7.

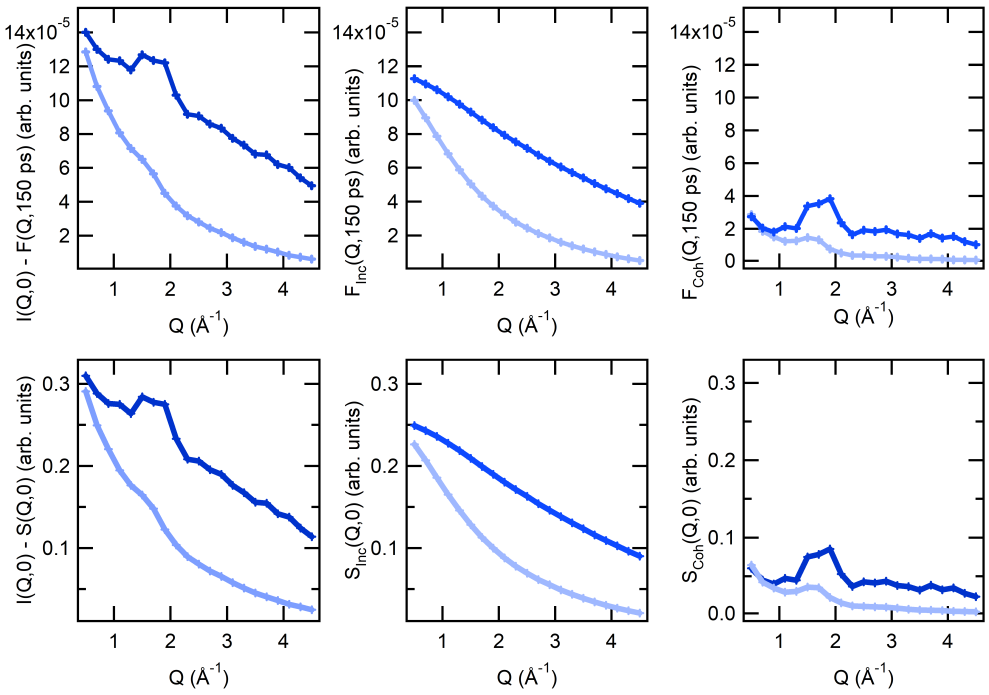

Fig. S7. $I(Q,0)$ **from numerical simulations.** Comparison between simulated neutron spectra $I(Q,0)$ calculated from the intermediate scattering functions at the experimental time resolution of 150 ps (upper panels) and from the total dynamical structure factors convoluted with the experimental resolution (lower panels) at 223 K (blue lines) and 293 K (light blue lines).The incoherent F_{Inc} and S_{Inc} are reported in the central panels of each row, while the coherent F_{Coh} and S_{Coh} contributions are shown in the rightmost panels.